



UNIVERSITY OF LEEDS

This is a repository copy of *Assessing eruption column height in ancient flood basalt eruptions*.

White Rose Research Online URL for this paper:
<http://eprints.whiterose.ac.uk/109782/>

Version: Accepted Version

Article:

Glaze, LS, Self, S, Schmidt, A orcid.org/0000-0001-8759-2843 et al. (1 more author)
(2017) *Assessing eruption column height in ancient flood basalt eruptions*. *Earth and Planetary Science Letters*, 457. pp. 263-270. ISSN 0012-821X

<https://doi.org/10.1016/j.epsl.2014.07.043>

© 2016 Elsevier B.V. and United States Government as represented by the Administrator of the National Aeronautics and Space Administration. Published by Elsevier B.V. This manuscript version is made available under the CC-BY-NC-ND 4.0 license
<http://creativecommons.org/licenses/by-nc-nd/4.0/>

Reuse

Unless indicated otherwise, fulltext items are protected by copyright with all rights reserved. The copyright exception in section 29 of the Copyright, Designs and Patents Act 1988 allows the making of a single copy solely for the purpose of non-commercial research or private study within the limits of fair dealing. The publisher or other rights-holder may allow further reproduction and re-use of this version - refer to the White Rose Research Online record for this item. Where records identify the publisher as the copyright holder, users can verify any specific terms of use on the publisher's website.

Takedown

If you consider content in White Rose Research Online to be in breach of UK law, please notify us by emailing eprints@whiterose.ac.uk including the URL of the record and the reason for the withdrawal request.



eprints@whiterose.ac.uk
<https://eprints.whiterose.ac.uk/>

1
2
3
4 **Assessing eruption column height in**
5 **ancient flood basalt eruptions**
6

7
8 Lori S. Glaze^a, Stephen Self^{b,c}, Anja Schmidt^d, and Stephen J. Hunter^d
9

10
11
12 ^aCode 690, NASA Goddard Space Flight Center, 8800 Greenbelt Road
13 Greenbelt, MD 20771, United States
14 Lori.S.Glaze@nasa.gov
15

16
17 ^bThe Open University, Department of Environment, Earth & Ecosystems, Walton Hall
18 Milton Keynes, MK7 6AA, United Kingdom
19 Steve.self1815@gmail.com
20

21
22 ^cUniversity of California, Berkeley, Earth and Planetary Science, 307 McCone Hall
23 Berkeley, CA 94720-9980, United States
24

25 ^dUniversity of Leeds, School of Earth and Environment,
26 Leeds, LS2 9JT, United Kingdom
27 A.Schmidt@leeds.ac.uk
28 S.Hunter@leeds.ac.uk
29

30
31
32 Corresponding Author: Lori S. Glaze, (1) 301-614-6466
33
34
35
36
37

38 Re-Submitted to EPSL
39 15 July 2014

40 *Abstract:* A buoyant plume model is used to explore the ability of flood basalt eruptions to
41 inject climate-relevant gases into the stratosphere. An example from the 1986 Izu-Oshima
42 basaltic fissure eruption validates the model's ability to reproduce the observed maximum plume
43 heights of 12 – 16 km above sea level, sustained above fire-fountains. The model predicts
44 maximum plume heights of 13 – 17 km for source widths of between 4 – 16 m when 32% (by
45 mass) of the erupted magma is fragmented and involved in the buoyant plume (effective volatile
46 content of 6wt%). Assuming that the Miocene-age Roza eruption (part of the Columbia River
47 Basalt Group) sustained fire-fountains of similar height to Izu-Oshima (1.6 km above the vent),
48 we show that the Roza eruption could have sustained buoyant ash and gas plumes that extended
49 into the stratosphere at $\sim 45^{\circ}\text{N}$. Assuming 5 km long active fissure segments and 9000 Mt of
50 SO_2 released during explosive phases over a 10-15 year duration, the ~ 180 km of known Roza
51 fissure length could have supported ~ 36 explosive events/phases, each with a duration of 3 - 4
52 days. Each 5 km fissure segment could have emitted 62 Mt of SO_2 per day into the stratosphere
53 while actively fountaining, the equivalent of about three 1991 Mount Pinatubo eruptions per day.
54 Each fissure segment could have had one to several vents, which subsequently produced lava
55 without significant fountaining for a longer period within the decades-long eruption. Sensitivity
56 of plume rise height to ancient atmospheric conditions is explored. Although eruptions in the
57 Deccan Traps (~ 66 Ma) may have generated buoyant plumes that rose to altitudes in excess of
58 18 km, they may not have reached the stratosphere because the tropopause was substantially
59 higher in the late Cretaceous. Our results indicate that some flood basalt eruptions, such as Roza,
60 were capable of repeatedly injecting large masses of SO_2 into the stratosphere. Thus sustained
61 flood basalt eruptions could have influenced climate on time scales of decades to centuries but

62 the location (i.e., latitude) of the province and relevant paleoclimate is important and must be
63 considered.

64

65 *Keywords: flood basalt; climate; Roza; sulfur dioxide; Columbia River Basalt Group; plume*
66 *heights*

67

68

69 **1. Introduction**

70 There is an intriguing age correlation between several continental flood basalt (CFB)
71 provinces emplaced in the past 300 Ma with mass extinction events (e.g., Wignall, 2001;
72 Courtillot and Renne, 2003; Kelley, 2007). The link between CFB volcanism and mass
73 extinctions may be due to gas release from the magmas or magma-sediment interactions
74 potentially leading to environmental changes (Self et al., 2014, Schmidt et al., 2014). Recent
75 studies have shed light on variations in eruption rate over time and the spatial distribution of
76 eruptive vents for the 14.7 Ma Roza Member of the Columbia River Basalt Group (CRBG) (e.g.,
77 Brown et al., 2014). These new data allow more robust assessment of magmatic gas
78 contributions to the atmosphere by CFB volcanism.

79 The effects of volcanism on climate are complex and occur over a range of time scales, from
80 days to possibly centuries (Robock, 2000; Timmreck, 2012). Sulfur species (sulfur dioxide, SO₂,
81 and hydrogen sulfide, H₂S) are the primary volcanic volatiles known to impact climate. Most
82 basaltic eruptions release SO₂ (Sharma et al., 2004) and most is known about its relevance for
83 climate when injected into the stratosphere. Sulfuric acid (H₂SO₄) aerosols derived from SO₂ and
84 H₂S can have long residence times (1 – 3 years) in the stratosphere, where these particles scatter

85 and absorb incoming solar and thermal infrared radiation, resulting in a net cooling at the surface
86 (e.g., Robock, 2000). Release of volcanic CO₂ may have a limited effect on climate (Self, et al.,
87 2006). However, magmatic interaction with sediments, may also play a role (Self et al., 2014).

88 Examples of large, historic, silicic explosive eruptions that have impacted climate on the 1–2
89 year timescale through the injection of large amounts of SO₂ into the stratosphere include
90 Tambora (1815), Krakatau (1883), Agung (1963), El Chichón (1982), and Pinatubo (1991). The
91 high-latitude (65°N) basaltic fissure eruption of Laki in 1783-1784 (Thordarson and Self, 1993;
92 Schmidt et al. 2010) injected SO₂ into the upper troposphere and lower stratosphere through
93 repeated sub-Plinian explosive phases over a period of eight months, affecting climate in the
94 northern hemisphere for up to two years (Thordarson et al., 1996; Highwood and Stevenson,
95 2003; Oman et al., 2006a; 2006b; Schmidt et al., 2012).

96 Masses of SO₂ injected into the atmosphere by historic explosive volcanic eruptions range
97 from ~ 7 Mt (= 7 Teragram) by El Chichón in 1982 (Bluth et al., 1992), to ~ 20 Mt by Pinatubo
98 in 1991 (Bluth et al., 1992), and ~ 60 Mt by Tambora in 1815 (Self et al., 2004). Up to 122 Mt of
99 SO₂ was emitted by the Laki eruption (Thordarson, et al., 1996), with over 90 Mt injected into
100 the upper troposphere and lower stratosphere over a 5 month period. Volcanic eruptions are also
101 capable of redistributing large volumes of water from the lower atmosphere into the stratosphere
102 (Glaze et al., 1997). Models indicate that a 25 km-high eruption column rising through a wet,
103 tropical atmosphere can transport up to 4 Mt of H₂O per hour. (“Plume” describes the vertical
104 eruption column and downwind ash/gas cloud.) In this case, ~30% of the water vapor in the
105 plume at its maximum height is derived from the erupted magma and ~70% is entrained while
106 passing through the moist lower atmosphere (Glaze et al., 1997).

107 Based on the atmospheric and environmental impacts observed following the Laki eruption,
108 some have speculated that large CFB eruptions (e.g., CRBG, peak 16-15 Ma; Deccan Traps peak
109 ~ 67-65 Ma) may have supplied large masses of SO₂ and other gases to the upper troposphere, or
110 possibly even the stratosphere (e.g., Stothers et al., 1986; Woods, 1993a; Thordarson and Self,
111 1996; Chenet et al., 2005; Self et al., 2005). Early attempts by Stothers et al. (1986) and Woods
112 (1993a) at modeling CFB plumes suggested that near-stratospheric heights could be attained by
113 high-intensity basaltic eruptions but there were many simplifications. CFB lava flow-fields, each
114 the product of one sustained eruption over decadal time-scales, are made up of multiple lava
115 flows that are proposed to have erupted with volumetric flow rates similar to the maximum
116 estimated for Laki (e.g., Self et al., 1998; Self et al., 2006). Long-duration effusive basaltic
117 eruptions, such as the current >30 year eruption of Pu`u `Ō`ō, Hawaii, are consistent with much
118 larger CFB events that may have been active over decades to possibly hundreds of years. These
119 larger CFB events may have injected as much as 1000 Mt of SO₂ into the atmosphere annually
120 (Self et al., 2005). Despite the long overall duration of CFB province emplacement (1 to a few
121 Ma), it is likely that this activity was characterized by long periods of inactivity, punctuated by
122 shorter duration eruptive phases lasting decades to possibly centuries.

123 We investigate the possible delivery of climate-relevant gases (SO₂ and H₂O) into the
124 atmosphere from CFB eruptions by combining numerical modeling and volcanological datasets
125 for the 14.7 Ma Roza flow of the CRBG (Thordarson et al., 1996; Brown et al., 2014). In
126 particular, we place constraints on the mass of SO₂ that such eruptions could have injected into
127 the stratosphere. This is the first application of a buoyant plume model to ash and gas plumes
128 sustained above a fire-fountain.

129

130 **2. Basaltic gas-ash plumes**

131 The key to having an impact on climate for a basaltic eruption is the ability to loft climate-
132 relevant gases into the stratosphere and to sustain the supply over many years, even
133 intermittently. Although not common, sustained buoyant plumes associated with large basaltic
134 fire-fountain events have been observed. An example is the Pu`u `Ō`ō eruption at Kilauea,
135 Hawaii (Figure 1); early episodes of the eruption in 1983 and 1984 generated fire-fountains, with
136 typical heights of 100–200 m, and occasionally as high as ~400 m (Wolfe et al., 1988), which
137 sustained gas and ash plumes of 5-7 km height above sea level (ASL). The 1984 eruption of
138 Mauna Loa, Hawaii, produced somewhat larger fire-fountains (up to 500 m high) along a 2 km-
139 long active fissure that generated a buoyant plume estimated to rise to 11 km ASL (7.5 km above
140 the vent) (Smithsonian Institution, 1984). Much larger fire-fountains were documented during
141 the 1986 eruption of Izu-Oshima, Japan, and, indirectly, the 1783-1784 eruption of Laki, Iceland.
142 At Izu-Oshima, fire-fountains 1.6 km high were observed to feed an ashy sub-Plinian plume that
143 reached 16 km ASL (Endo et al., 1988; Sumner, 1998; Mannen and Ito, 2007). Miyakejima,
144 Japan, also produced 12-km-high plumes during a basaltic fissure eruption in 1983, but the exact
145 source of the plumes is not known (Aramaki et al., 1986). Fire-fountains at Laki, estimated to
146 have reached 0.8 – 1.4 km in height, were observed from afar to sustain eruption columns of up
147 to 15 km altitude (Thordarson and Self, 1993; Oman et al., 2006a). These historic eruptions can
148 be used to evaluate plume-rise models for application to convecting, buoyant ash plumes
149 sustained above fire-fountains.

150

151 **3. Modeling plume rise above fire-fountains**

152 Buoyant plume dynamics play an important role in the ability of explosive volcanic eruptions
153 to supply climate-relevant gases to the atmosphere. Several models are available for buoyant
154 plume rise from a central vent (e.g., Woods, 1988; Woods, 1993b; Glaze et al., 1997; Mastin,
155 2007) or linear vent (Stothers et al., 1986; Stothers, 1989; Woods 1993a; Glaze et al., 2011). The
156 results of these studies are largely contained in two comprehensive models, *Plumeria* (Mastin,
157 2007) and *4C* (Glaze et al., 1997). However, the Woods (1988; 1993b) model, upon which
158 *Plumeria* is based, includes two fundamental inconsistencies in the formulation, resulting in key
159 differences with *4C* (Glaze and Baloga, 1996; Glaze, 1999). The net effect of these differences
160 is a 4-7% overestimate of maximum plume height using the Woods (1988; 1993b) approach (see
161 Appendix).

162 For plumes with large mass flux, the dynamics are almost completely dominated by the
163 buoyancy driven region. Thus, the *4C* model as used here is focused on the buoyancy-driven
164 regime and does not include a “jet region” near the vent, as defined by Woods (1988). This is
165 consistent with modeling ash-gas plumes that are driven by fire-fountains (or even roiling lava
166 lakes) as the starting point: the plume of interest is essentially a “hot-plate zone” of semi-
167 consistent height (usually ≤ 1.5 km above the local surface for a big fountain).

168 The basic input data required for *4C* are the mass flux (defined by the source area, and
169 eruption velocity), eruption temperature, and gas mass fraction of the erupting magma.
170 Variations in the atmospheric temperature and pressure may also affect estimated maximum
171 plume heights (Woods, 1993b; Glaze et al., 1997; Glaze, 1999; Glaze and Baloga, 1996). For
172 applications to ancient eruptions, small variations in atmospheric composition, for example,
173 differences in CO₂ concentrations between 65 Ma ago (if modeling the Deccan Traps eruptions)
174 and now, may also influence atmospheric temperature structure, and thus predicted plume

175 behavior (see Section 6.1). The primary 4C model output is predicted maximum plume height
176 along with mass fluxes of water and SO₂ at the maximum plume height altitude.

177 Buoyant plumes driven by basaltic fire-fountains differ from most other explosive volcanic
178 plumes in that most of the solid material falls immediately back to the surface. The resulting
179 plumes are, therefore, relatively gas-rich (i.e., ash-poor) in comparison to their more silicic
180 counterparts. Typical values for bulk magma volatile contents range from 2–5wt%. However,
181 gas fractions of 70–94wt% have been measured in explosive basaltic “bursts” at Stromboli
182 (Chouet et al., 1974).

183 Figure 2 illustrates the importance of ash on maximum rise height. The simplest case is a
184 steam plume with temperature of 100 °C, and initial velocity of 50 m/s. The maximum plume
185 height is increased 25-30% by increasing the eruption temperature to 925°C (thus increasing the
186 density difference driving buoyancy). Addition of a relatively small amount of ash to the plume
187 (50wt% compared with 95-98wt% in a typical explosive silicic eruption; where ash particles are
188 4-5 orders of magnitude more dense than gas) increases the mass flux at the source (keeping the
189 vent size the same) and results in an overall increase in maximum plume height. In addition to
190 increasing the mass flux (known to be correlated with maximum height, e.g., Sparks et al., 1997),
191 solid particles have a much higher heat capacity than water vapor, resulting in the ability to keep
192 the plume warm and buoyant, despite the higher initial bulk plume density.

193 One of the keys to modeling the behavior of buoyant plumes is to estimate the relative
194 amounts of ash and volatiles in the plume. Previous studies (Stothers, 1989; Woods, 1988;
195 1993a; 1993b; Glaze et al., 1997; 2011) have used bulk magmatic volatile contents (~2-5wt%).
196 However, for ash plumes sustained above fire-fountains, this approach will underestimate the
197 ratio of volatiles to solid ash. To better estimate this ratio, there are two processes to consider.

198 First, because it is easier for volatiles to separate from the melt phase in basaltic magmas than
199 from more silicic magmas (Sparks and Pinkerton, 1978), basaltic magmas may de-gas over time,
200 producing a gas-rich layer trapped at the top of the magma body (Vergnolle and Mangan, 2000;
201 Houghton and Gonnermann, 2008). Bonaccorso et al. (2011) indicate that the magma volume
202 required to provide the SO₂ observed during a Mt. Etna fire-fountain event would have needed to
203 be 10 times the amount of all the erupted magma (effusive plus explosive). They note that other
204 styles of volcanic activity with longer repose times (months to years) have ratios more like 4 to 1
205 of degassed to erupted magma. This implies that gas erupted with the explosive phase was
206 derived from a magma volume that is considerably larger than the combined volume of erupted
207 lava and ash. Thus, models of buoyant plume rise from basaltic eruptions may need to allow for
208 a volatile content that is greater than the bulk magmatic value.

209 The second consideration is that much of the erupted lava from a fire-fountain returns to the
210 ground and does not participate in the buoyant plume. Kaminski et al. (2011b) propose a
211 mechanism for partitioning erupted magma between that which is lofted by the buoyant plume
212 and that which is not (effusive flows and fire-fountain material that immediately falls back to the
213 surface) by defining a parameter, f , the “fraction of magma finely fragmented and injected into
214 the plume”. The f parameter has a single value that determines the mass flux boundary condition
215 for solid material into the plume at the source. For magma with a bulk volatile content of
216 $n_o=3\text{wt}\%$, and all the associated magma explosively released concurrently with the gas forming a
217 buoyant ash plume, $f=1$ and the mass fraction of solids in the plume is $(1 - n_o)=97\text{wt}\%$. If,
218 however, only a fraction of the erupted magma contributes to the buoyant plume, the new
219 “effective” volatile content is (Kaminski et al., 2011b),

$$n_f = \frac{n_o}{n_o + f(1 - n_o)}$$

220 For example, if the mass of lava erupted as lava flows and fire-fountains is twice that which
221 makes up the buoyant plume (lava+fire-fountain=66.66%, plume=33.33% of total erupted mass),
222 then $f=33.33\%$. For $n_o=3\text{wt}\%$, the effective volatile content becomes, $n_f=8.5\text{wt}\%$, almost three
223 times higher than the bulk volatile content of 3wt%. The observations of Chouet et al. (1974) are
224 consistent with ash-poor buoyant plumes associated with intermittent basaltic fire-fountains and
225 even higher values of n_f . Based on the observations reported by Bonaccorso et al. (2011), if the
226 ratio of degassed to erupted magma is 4 to 1, and the mass fraction of solid material in the plume
227 to the total erupted mass is 3%, then $f=3\% * 25\%=0.75\%$, and $n_f=80\text{wt}\%$ (for $n_o=3\text{wt}\%$). This is
228 consistent with the Chouet et al. (1974) observations of 70–94wt% volatiles in Strombolian fire-
229 fountains. Values for f can range from 0–100%, however, for a fire-fountain to sustain a buoyant
230 ash plume a substantial fraction of solid material must be incorporated into the plume. A detailed
231 study of the minimum f to sustain a buoyant ash plume is reserved for future study. It can be
232 estimated, however, that the 1986 Izu-Oshima and the Laki fire-fountain eruptions, which both
233 sustained large ash plumes, erupted ~30-35% of the magmatic mass as tephra ($f=30\text{-}35\%$, see
234 discussions below).

235

236 **4. Model validation for 1986 Izu-Oshima eruption**

237 The 1986 eruption of Izu-Oshima, Japan, produced some of the largest documented basaltic
238 fire-fountains. Fire-fountains from the Izu-Oshima “B” fissure reached a maximum height in
239 excess of 1600 m (above the vent) (Endo et al., 1988; Sumner, 1998). At their most energetic,
240 the fire-fountains sustained a sub-Plinian buoyant ash plume that reached 12–16 km ASL

241 (Mannen, 2006; Mannen and Ito, 2007). The vent system for this eruption was made up of eight
242 vents distributed along four en echelon fissure segments (Endo et al., 1988; Sumner, 1998). At
243 the climax of the B eruption, lava fountains were observed from all vents between B3 and B8 (~1
244 km of fissure length).

245 Assuming ballistic physics of a vertical projectile, the maximum height of fire-fountain
246 material can be found from $y=y_o+(v^2-v_o^2)/(2g)$, where y_o and y are the initial and final altitudes, v_o
247 and v are the initial and final velocities, and $g=-9.8 \text{ m/s}^2$ is gravitational acceleration (e.g.,
248 Resnick and Halliday, 1977). For a fire-fountain with $(y - y_o)=1600 \text{ m}$ and velocity at the apex of
249 $v=0$, this implies an ejection velocity (at the vent, v_o) of ~175 m/s. At some point within the fire-
250 fountain, the fine-grained ash and gas components dynamically separate from the ballistic
251 material (which falls back to the surface). Lacking data on where this dynamic separation
252 occurs, we assume that the gas and fine-grained ash that form the buoyant plume separate from
253 the fire-fountain about 1000 m above the vent (~2/3 of the maximum fountain height), and begin
254 modeling the buoyant convective plume at this point. Using the same expression for ballistic
255 physics, the velocity is ~100 m/s at $y=1000 \text{ m}$. The Izu-Oshima B-vents extend from ~500–600
256 m elevation (Smithsonian Institution, 1986). Thus, the buoyant plume model is initiated at an
257 altitude of 1500 m (1000 m above the vent). A velocity of 100 m/s is assumed at the starting
258 point of buoyant plume rise. Fire-fountains are generally still “red hot” at the apex. In the
259 absence of data on lava temperatures during the Izu-Oshima eruption, the temperature of the
260 buoyant plume material at the point where it separates from the fire-fountain is assumed to be
261 ~1075 °C. The model is not sensitive to choice of initial velocity and reducing the starting
262 temperature by as much as 150 °C has minimal effect on the overall plume rise.

263 Entrainment dynamics in the lower part of the buoyant plume are more efficient for a linear
264 vent than a central vent (Sparks et al., 1997; Glaze et al., 2011), and can have an effect on overall
265 plume rise. Figure 3 shows the maximum height achieved by buoyant plumes from three
266 combinations of vent size and geometry. The x-axis shows a range of effective gas contents from
267 very ash-poor, $n_f = 80\text{wt}\%$ ($f=0.5\%$, $n_o=2\text{wt}\%$) to ash-rich examples, $n_f = 10\text{wt}\%$ ($f=18\%$,
268 $n_o=2\text{wt}\%$).

269 Fire-fountains during the early days of the Pu'u Ō'ō eruption ranged from 200–400 m high.
270 Images in Wolfe (1988) indicate these fire-fountains had widths of ~50–100 m. A circular
271 source with diameter of 50 m is shown in Figure 3. It can be seen that for this 'typical' fire-
272 fountain geometry, ash-poor plumes are only capable of rising to about 6 km, consistent with
273 buoyant plumes observed above Pu'u Ō'ō fire-fountains. Increasing the relative amount of ash
274 released with the gas drives the plume higher, but the plume does not reach the minimum 12 km
275 ASL observed at Izu-Oshima, even if all erupted magma is incorporated into the rising plume.

276 Doubling the source diameter to 100 m (not shown) can produce a sustained plume that
277 almost reaches 12 km ASL, but only for $n_f \ll 10\text{wt}\%$, where essentially all of the erupted
278 material is incorporated into the buoyant plume. Assuming $f \approx 100\%$ is not consistent with
279 observations of the Izu-Oshima fire-fountains where Sumner (1998) reports clastogenic lava
280 flows, indicating that a substantial proportion of the fire-fountain material was still hot and fluid
281 enough to remobilize after returning to the ground. Thus, circular-vent boundary conditions are
282 not able to produce a sustained buoyant plume of the scale observed during the eruption.

283 Figure 3 also shows estimated plume heights for a linear source that is 1 km long (as
284 observed at Izu Oshima) and 4 m wide or 16 m wide. For the 16 m wide linear source, the

285 effective volatile contents that result in a sustained plume between 12-16 km range from
286 relatively ash-poor ($n_f=50\text{wt}\%$) to ash rich ($n_f=10\text{wt}\%$). The Izu-Oshima eruption phases from
287 the B-vents produced 3.0×10^{10} kg of lava (in the form of lava flows and scoria cones) and $1.4 \times$
288 10^{10} kg tephra (transported by the buoyant plume) (Endo et al. (1988). This results in $f=32\%$ and
289 $n_f=6\text{wt}\%$ (for $n_o=2\text{wt}\%$). The two linear source widths shown in Figure 3 result in predicted
290 plume heights between 13.1 – 17.4 km ASL for $n_f=6\text{wt}\%$, consistent with the range of observed
291 buoyant plume heights.

292

293 **5. Results and implications for the Roza eruption**

294 The 14.7 Ma Roza flow (CRBG) comprises 1300 km^3 of lava erupted from a 180-km-long
295 vent system, and has the best described fissure flood-basalt vent system in the world.
296 Thordarson and Self (1998) suggest that the Roza eruption involved multiple phases over a
297 period of ten to several tens of years. Evidence from pyroclastic deposits indicates multiple
298 vents along the 180 km fissure system (Swanson et al., 1975), with a minimum of 11 identified
299 vents in the northern-most 32 km (Brown et al., 2014).

300 Brown et al. (2014) show that eruptive activity at the northerly Roza vents began with a more
301 explosive phase, followed by effusion of large-volume lava flows with less or little attendant
302 explosive activity. Observations of historic basaltic fissure eruptions indicate that active linear
303 vents are generally limited to lengths of no more than a few kilometers (e.g., Walker et al., 1984;
304 Thordarson and Self, 1993), and generally contract down to centralized vents within a short
305 period of time (Bruce and Huppert, 1989). Fissure lengths of 1 - 5 km are considered here.
306 Although the active-fissure length does not affect the predicted plume heights (Glaze et al.,
307 2011), it will have a substantial influence on the mass of material delivered to the plume top.

308 To estimate the likely plume rise height for the Roza eruption we assume parameters
309 analogous to Izu-Oshima (fissure width=4-16 m, eruption temperature=1075 °C, starting
310 velocity=100 m/s). Based on glass inclusion data (Thordarson and Self, 1996), a bulk Roza
311 volatile content of 2wt% is assumed. As for Izu-Oshima, we assume the buoyant column
312 separates from the fire-fountain ~1000 m above the vent. The current Roza vent elevation is ~
313 550 m ASL. However, incision of the Snake River Canyon indicates that the region has likely
314 been uplifted by several hundred meters since 15 Ma ago. Thus, an initial vent elevation of 200
315 m is assumed here, resulting in a plume source altitude of 1200 m. The 300 m difference in
316 initial altitude (compared to Izu Oshima) results in a small difference of <0.1 km in overall rise
317 height.

318 Because of the similarity to the Izu Oshima example, the range of maximum plume heights
319 for the Roza eruption is 13.1–17.4 km ASL for fissure widths of 4-16 m (as shown in Figure 3).
320 At Roza's ~45°N paleo-latitude the tropopause is between 10–13 km ASL, depending on season.
321 Thus, a plume from a 16 m wide linear source ($f \sim 32\%$, $n_f=6\text{wt}\%$), can easily drive a plume into
322 the stratosphere (Figure 3), even for more ash-poor cases. In order to assess the possible
323 atmospheric impact of the Roza eruption, we can examine the volumes of magmatic volatiles
324 that are injected into the stratosphere at the maximum plume height. Lacking specific total
325 magmatic volatile information for Roza, we have assumed an example bulk magmatic volatile
326 composition based on compositions of Kilauea lavas from Gerlach (1980), with 42% H₂O; 15%
327 CO₂; 43% SO₂.

328 The total mass flux of material (gas plus ash) into the buoyant plume from a 16 m wide linear
329 source is 5,567 kg/s per meter of fissure length. For $n_f=6\text{wt}\%$, and a volatile content analogous to
330 Kilauea, the mass flux of SO₂ is 144 kg/s per meter of fissure length. Thus, this plume could

331 release 12.4 Mt of SO₂ per day for each kilometer of active fissure. If an eruptive episode began
332 with an explosive phase along a 5 km segment of fissure, that phase could inject 62 Mt per day
333 of SO₂ into the stratosphere, the equivalent of about three 1991 Pinatubo eruptions each day.

334 Thordarson and Self (1996) report a total of >12,400 Mt of SO₂ potentially released by the
335 Roza eruption, with >9000 Mt of SO₂ emitted during explosive phases. At a rate of 62 Mt of
336 SO₂ per day (per 5 km segment), it would take ~ 145 days of explosive activity (distributed
337 throughout the decades-long eruption) to release 9000 Mt of SO₂. Assuming 5 km-long active
338 fissure segments, the 180+ km of known fissure length could thus have supported ~ 36 explosive
339 events, each with duration of 3 - 4 days of intense fire-fountaining.

340

341 **6. Discussion**

342 The model applications above assume that the atmospheric composition and
343 temperature/pressure profiles 15 Ma ago (Miocene) were similar to the modern atmosphere.
344 However, much older CFB provinces, e.g., Deccan Traps, India (~66 Ma), likely erupted into a
345 substantially different atmosphere. A sensitivity study is provided here to assess the influence of
346 atmospheric temperature structure and tropopause height, based on increased CO₂
347 concentrations, on predicted plume rise heights. We also explore an alternative to convective
348 rise above fire-fountains where hot volcanic gases released from massive sheet flows covering
349 large areas combine with warmed air above the flows forming a convective plume (Kaminski et
350 al., 2011a).

351

352 **6.1 Implications for plume rise in ancient atmospheres**

353 To test the sensitivity of plume rise heights to atmospheric conditions representative of the
354 Late Cretaceous and Miocene we have used climate simulations based on the HadAM3
355 Atmosphere-only climate model (Pope et al., 2000). This model has been extensively used and
356 evaluated in Cretaceous (including Craggs et al., 2012; Hunter et al., 2013) and Miocene studies
357 (Lunt et al., 2008; Pound et al., 2011). The model has $2.5^{\circ} \times 3.75^{\circ}$ horizontal resolution and 19
358 unevenly spaced layers in the vertical (up to 39 km). For the Maastrichtian we use the 71.3-65.0
359 Ma time-slice, 1120 ppmv CO₂ control experiment of Hunter et al. (2013). The Miocene
360 experiment represents a 11.6-7.3 Ma time-slice with 395 ppmv CO₂ (Pound, 2012). Both
361 experiments assume a modern orbit and pre-industrial atmospheric composition (except for
362 CO₂). Model integration length is sufficient to ensure surface climatology has attained
363 equilibrium. Vertical profiles of pressure, temperature and specific humidity are averaged from
364 the final 30 model years and linearly interpolated to 500 m grid cells. Based on the standard
365 World Meteorological Organization (WMO) lapse-rate criterion, we calculate the tropopause
366 height as the “lowest level at which the lapse-rate decreases to 2°C/km or less, provided that the
367 average lapse-rate between this level and all higher levels within 2 km does not exceed 2°C/km”
368 (WMO, 1957).

369 *4C* has been run using the Roza boundary conditions (Section 5), but replacing the
370 atmosphere with Miocene definitions for temperature (Figure 4). The Miocene pressure profile
371 does not differ substantially from the modern atmosphere. The resulting range of maximum
372 plume heights is 12.2 – 16.5 km (fissure widths of 4 and 16 m, respectively). Both ends of this
373 range are shifted downward by 0.9 km relative to results using the modern atmosphere. Although
374 the effect is relatively small, this systematic behavior is attributed to the warmer troposphere in
375 the mid-Miocene. In the HadAM3 model, the tropopause height of about 13 km at 45°N for the

376 Miocene is ~2 km higher than the pre-industrial/modern atmosphere. Thus, the ability of Roza-
377 like plumes to reach the stratosphere is somewhat sensitive to the choice of temperature profile.

378 This study can also be extended to explore possible buoyant plumes associated with fire-
379 fountains during the emplacement of the Deccan Traps that were coincident with the K-Pg mass
380 extinction (e.g., Wignall, 2001; Keller et al., 2012). The Maastrichtian atmospheric temperatures
381 differ significantly from the modern atmosphere, in part due to the increased levels of CO₂ (4
382 times pre-industrial concentration assumed here). Using the Maastrichtian atmosphere
383 temperature profile, and keeping all other boundary conditions the same, the predicted range of
384 maximum plume heights is 11.9 – 18.3 km (fissure widths of 4 and 16 m, respectively). The low
385 end of this range is lower and the high end is higher than for the modern atmosphere. The
386 broader range of maximum plume heights is primarily owing to differences in the shape of the
387 temperature profile compared with the US Standard temperature profile (Figure 4). At low
388 altitudes, the Maastrichtian atmosphere is warmer than the US Standard, meaning the density
389 difference (driving buoyancy) between the plume and ambient air is smaller and the plume will
390 stop rising sooner (a lower maximum rise height for 4 m fissure width). Above ~13 km altitude,
391 the US Standard atmosphere is significantly warmer than the Maastrichtian, which reduces the
392 density difference for the US Standard atmosphere. Plumes in the Maastrichtian atmosphere will
393 continue to rise a little higher in the cooler troposphere. Despite a higher buoyant rise in the
394 Maastrichtian atmosphere, at about 21°S (the paleo-latitude of the Deccan Traps) the tropopause
395 is shifted upward significantly to an altitude of about 20.5 km compared to about 16 km in the
396 modern atmosphere. Thus, based on the climate model predictions of tropopause height, it seems
397 unlikely that plumes originating from volcanic vents in the tropics of the size examined here
398 would have reached the stratosphere during the Maastrichtian. These results imply that the

399 chemical processing and the lifetime of volcanic gases and aerosol particles may differ for
400 different CFB provinces depending on atmospheric temperatures at the time of emplacement.

401 The influence of atmospheric composition on plume buoyancy was also considered. *4C*
402 assumes an atmospheric mol mass of 28.966 g/mol. Increasing atmospheric CO₂ concentrations
403 by a factor of four above pre-industrial levels, and keeping all other constituents the same, results
404 in a mol mass of 28.990 g/mol. This slight increase results in a bulk atmosphere gas constant for
405 the Maastrichtian of 286.8 J/kg/K, indistinguishable from 287.0 J/kg/K used in *4C*.

406

407 **6.2 Rise of plumes above lava lobes**

408 To model the rise of plumes above CFB flow fields, Kaminski et al. (2011a) considered
409 penetrative convection driven by cooling of large basaltic lava flows. While penetrative
410 convection is likely present and may somewhat increase predicted maximum plume heights, we
411 question whether there would be a sufficient area of hot lava to support a vigorous convective
412 plume above a flood basalt sheet lobe, or group of active lobes.

413 One issue not accounted for by Kaminski et al. (2011a) is that most (~ 75 % by mass) of the
414 magmatic gas released to the atmosphere comes from the vent, with the remainder released from
415 the lava flows (see summary in Thordarson et al. (2003)). Thus, by far the biggest release of gas
416 into the atmosphere is the plume above the vent. Moreover, even near the vents, the CFB lava
417 flow-fields are predicted to grow very gradually over years to decades (Self et al., 2005) and
418 seldom will there be areas with near-magmatic-temperatures bigger than a few 100 m² due to the
419 rapid development of a strongly insulating crust (Hon et al., 1994).

420 Another issue is the geometry with the vent in the middle of the CFB lava flow field
421 (Kaminski et al., 2011a). This does not occur often in CFB provinces, as the lava flows away
422 from the vent area, exemplified by the smaller Laki 1783-1784 analog (Thordarson and Self,
423 1993) and the distribution of the Roza flow (Brown et al., 2014). Further, the Van Dop et al.
424 (2005) experimental tank upon which the Kaminski et al. (2011a) hypothesis is partly based has
425 finite width and length. In contrast, the “well mixed” atmospheric boundary layer is infinitely
426 wide compared to the areal extent of the lava flow. Kaminski et al. (2011a) do not discuss the
427 importance of heat source area required to make this approach valid. The heat source areas
428 covered by flood basalt lava flows are small relative to those considered by Van Dop et al.
429 (2005), such as oceans.

430 Forest-fire pyro-cumulus clouds/plumes (pyro-Cbs) also provide an interesting comparison
431 with flood basalt eruption plumes, as they can reach the stratosphere without any “gas-thrust”
432 phase (Fromm et al., 2005; 2010). While forest-fire burn temperatures (~800-1000 °C) are a
433 little lower than magmatic basalt temperatures, they usually provide wide-area plume bases.
434 Many of the fires that generate pyro-Cbs cover 10s – 100s of thousands of hectares, one to two
435 orders of magnitude larger than the 3 – 20 km² of individual sheet lobes, or groups of co-
436 emplaced lobes, that make up the Roza member. With development of insulating upper crusts
437 (Self et al., 1998), this small area would not have been at “magmatic” temperatures. Thus it is
438 unlikely that the surface of flood basalt sheet lobes are hot enough to sustain vigorous
439 penetrative convection to great heights as suggested by Kaminski et al. (2011a).

440

441 **7. Conclusions**

442 Based on historical observations of large basaltic eruptions, buoyant plumes of gas and ash
443 could have been sustained above fire-fountains along the 14.7 Ma Roza fissure vent system.
444 Two modeling approaches are evaluated for predicting plume rise heights. Maximum plume
445 heights estimated by the *4C* model (Glaze et al., 1997; 2011) are comparable to those predicted
446 by the publicly available *Plumeria* model. However, *Plumeria* consistently overestimates
447 maximum plume heights by 4-7% owing to two inconsistencies in the Woods (1988; 1993b)
448 model upon which it is based: (1) discontinuous numerical solutions across the jet-buoyancy
449 transition, and (2) the thermal energy conservation term is not consistent with momentum
450 conservation.

451 Buoyant gas and ash plumes above an active fire-fountain are modeled using *4C* by
452 assuming, based on observations, that $\sim 2/3$ of the erupted magma returns to the surface. To
453 validate the model application to a buoyant plume fed by a fire-fountain, an example from the
454 1986 Izu-Oshima fissure eruption is examined. Linear source widths of 4 m and 16 m produce
455 maximum plume heights of 13.1 and 17.4 km ASL, respectively, that bracket the range of
456 observed heights (12 – 16 km ASL) for an effective volatile content of $n_f=6\text{wt}\%$, equivalent to a
457 bulk magma volatile content of $n_o=2\text{wt}\%$ and 32% of the erupted magma participating in the
458 buoyant plume as fragmented ash. A basaltic fissure eruption of the scale of Izu-Oshima can
459 easily drive a buoyant plume into the stratosphere, consistent with earlier work of Stothers et al.
460 (1986).

461 If the Roza eruption sustained fire-fountains of similar height to Izu-Oshima (1.6 km above
462 the vent), buoyant gas and ash plume heights of 13.1–17.4 km reaching the stratosphere at 45°N
463 could also be sustained. The primary scale differences between Izu-Oshima and Roza are the
464 possible lengths of active fissure and the duration of explosive activity. If an eruptive episode at

465 Roza began with an explosive phase along a 5 km fissure segment, that phase could inject 62 Mt
466 per day of SO₂ into the stratosphere; equivalent to SO₂ emissions from three 1991 Mount
467 Pinatubo eruptions each day. Assuming 5 km active fissure segments, the 180 km of known
468 fissure length could have supported ~36 explosive events each with duration of 3-4 days. Small
469 changes in the atmospheric temperature profile for the Miocene (relative to the modern
470 atmosphere) result in slightly lower predicted plume heights. Plumes erupted in the
471 Maastrichtian could have reached much higher into the atmosphere, but may not have extended
472 into the stratosphere owing to the higher tropopause in the late Cretaceous.

473 The plume heights and mass flux estimated here can be used as input for 3-D climate models
474 to quantify the effect on surface temperatures from eruptions such as Roza that consistently
475 injected SO₂ into the stratosphere on a periodic basis over many years. The Roza eruption
476 represents only one of ~ 120-150 members of the CRBG. Taking into account other eruptions in
477 the CRBG, it is possible that large-scale flood basalt eruptions could have had a substantial
478 influence on the chemistry of the atmosphere on timescales of decades to hundreds of years, and
479 consequently, on climate.

480

481 **Acknowledgements**

482 L. Glaze was funded by NASA Planetary Geology and Geophysics (WBS 811073.02.01.05.80)
483 and S. Self was funded by UK–NERC research grants NER/B/S/2003/00246 and GR3/11474 for
484 part of this research. A. Schmidt was funded by an Academic Research Fellowship from the
485 School of Earth and Environment, University of Leeds. We thank Steve Baloga and Luke Oman
486 for providing comments on an early version of this manuscript, and Tim Elliott, Laszlo Kestay,
487 and two anonymous reviewers for providing constructive reviews.

488 **References**

- 489 Aramaki, S., Hayakawa, Y., Jujii, T., Nakamura, K., Fukuoka T., 1986, The October 1983
490 eruption of Miyakejima volcano. *J. Volcanol. Geotherm. Res.* 29, 203-229.
- 491 Bluth, G.J.S., Doiron, S.D., Schnetzler, C.C., Krueger, A.J., Walter L.S., 1992, Global tracking
492 of the SO₂ clouds from the June, 1991 Mount Pinatubo eruptions. *Geophys. Res. Letts.*
493 19 (2), 151-154.
- 494 Bonaccorso, A., Caltabiano, T., Current, G., Del Negro, C., Gambino, S., Ganci, G.,
495 Giammanco, S., Greco, F., Pistorio, A., Salerno, G., Spampinato, S., Boshci E., 2011,
496 Dynamics of a lava fountain revealed by geophysical, geochemical and thermal satellite
497 measurements: The case of the 10 April 2011 Mt Etna eruption. *Geophys. Res. Letts.* 38
498 (L24307), doi:10.1029/2011GL049637.
- 499 Brown, R.J., Blake, S., Thordarson, T., Self, S., 2014, Pyroclastic edifices record vigorous lava
500 fountains during the emplacement of a flood basalt flow field, Roza member, Columbia
501 River Basalt Province, USA. *GSA Bull.*, doi:10.1130/B30857.1.
- 502 Bruce, P.M. and Huppert, H.E., 1989, Solidification and melting along dykes by the laminar flow
503 of basaltic magma, in: Ryan, M.P. (Ed.), *Magma Transport and Storage*. Wiley, New
504 York, 87 – 101.
- 505 Chenet, A.-L., Fluteau, F., Courtillot, V., 2005, Modelling massive sulphate aerosol pollution,
506 following the large 1783 Laki basaltic eruption. *Earth and Plan. Sci. Lett.* 236, 721-731.
- 507 Chouet, B., Hamisevicz, N., McGetchin, T.R., 1974, Photoballistics of volcanic jet activity at
508 Stromboli, Italy. *J. Geophys. Res.* 79, 4961 – 4976.
- 509 Courtillot, V.E., Renne, P.R., 2003, On the ages of flood basalt events, *Comptes Rendus*

510 Geoscience, 335, 113-140.

511 Craggs, H.J., Valdes, P.J., Widdowson, M., 2012, Climate model predictions for the latest
512 Cretaceous: An evaluation using climatically sensitive sediments as proxy indicators.
513 Palaeogeography, Palaeoclimatology, Palaeoecology, 315-316, 12-23.

514 Endo, K., Chiba, T., Taniguchi, H., Sumita, M., Tachikawa, S., Miyahara, T., Uno, R., Miyaji,
515 N., 1988, Tephrochronological study on the 1986-1987 eruptions of Izu-Oshima volcano,
516 Japan. *Volcanol. Soc. Japan* 2 (33), S32-S51.

517 Fromm, M., Bevilacqua, R., Servranckx, R., Rosen, J., Thayer, J.P., Herman, J., Larko, D., 2005,
518 Pyro-cumulonimbus injection of smoke to the stratosphere: Observations and impact of a
519 super blowup in northwestern Canada on 3-4 August 1998. *J. Geophys. Res.* 110,
520 doi:10.1029/2004JD005350.

521 Fromm, M., Lindsey, D.T., Servranckx, R., Yue, G., Trickl, T., Sica, R., Doucet, P., Godin-
522 Beekmann, S., 2010, The untold story of pyrocumulonimbus. *Bull. Am. Met. Soc.* 91,
523 1193-1209, doi:10.1175/2010BAMS3004.1.

524 Gerlach, T.M., 1980, Evaluation of volcanic gas analyses from Kilauea volcano. *J. Volcanol.*
525 *Geotherm. Res.* 7, 295-317.

526 Glaze, L.S., 1999, Transport of SO₂ by explosive volcanism on Venus. *J. Geophys. Res.* 104
527 (E8), 18,899 - 18,906.

528 Glaze, L.S., Baloga, S.M., 1996, Sensitivity of buoyant plume heights to ambient atmospheric
529 conditions: Implications for volcanic eruption columns. *J. Geophys. Res.* 101 (D1) 1529-
530 1540.

- 531 Glaze, L.S., Baloga, S.M., Wilson, L., 1997, Transport of atmospheric water vapor by volcanic
532 eruption columns. *J. Geophys. Res.* 102 (D5), 6099 – 6108.
- 533 Glaze, L.S., Baloga, S.M., Wimert, J., 2011, Explosive volcanic eruptions from linear vents on
534 Earth, Venus and Mars: Comparisons with circular vent eruptions. *J. Geophys. Res.* 116
535 (E01011), doi:10.1029/2010JE003577.
- 536 Highwood, E. J., and Stevenson, D. S., 2003, Atmospheric impact of the 1783-1784 Laki
537 Eruption: Part II - Climatic effect of sulphate aerosol: *Atmos. Chem. Phys.* 3, 1177-1189.
- 538 Hon, K., Kauahikaua, J., Denlinger, R., Mackay, K., 1994, Emplacement and inflation of
539 pahoehoe sheet flows: Observations and measurements of active lava flows on Kilauea
540 Volcano, Hawaii. *Geol. Soc. Am. Bull.* 106, 351-370.
- 541 Houghton, B.F., Gonnermann, H.M., 2008, Basaltic explosive volcanism: Constraints from
542 deposits and models. *Chemie der Erde* 68, 117-140.
- 543 Hunter, S.J., Haywood, A.M., Valdes, P.J., Francis, J.E., Pound, M.J., 2013, Modeling equable
544 climates of the Late Cretaceous: Can new boundary conditions resolve data-model
545 discrepancies? *Palaeogeography, Palaeoclimatology, Palaeoecology* 392, 41-51.
- 546 Kaminski, E., Chenet, A.-L., Jaupart, C., Courtillot, V., 2011a, Rise of volcanic plumes to the
547 stratosphere aided by penetrative convection above large lava flows. *Earth and Plan. Sci.*
548 *Lett.* 301, 171–178.
- 549 Kaminski, E., Tait, S., Ferrucci, F., Martet, M., Hirn, B., Husson, P., 2011b, Estimation of ash
550 injection in the atmosphere by basaltic volcanic plumes: The case of the Eyjafjallajokull
551 2010 eruption. *J. Geophys. Res.* 116 (B00C02), doi:10.1029/2011JB008297.
- 552 Keller, G., Adatte, T., Bhowmick, P. K., Upadhyay, H., Dave, A., Reddy, A. N., and Jaiprakash,

553 B. C., 2012, Nature and timing of extinctions in Cretaceous-Tertiary planktic
554 foraminifera preserved in Deccan intertrappean sediments of the Krishna–Godavari
555 Basin, India: *Earth and Planetary Science Letters*, v. 341–344, p. 211-221.

556 Kelley, S., 2007, The geochronology of large igneous provinces, terrestrial impact craters, and
557 their relationship to mass extinctions on Earth, *J. Geol. Soc.*, 164, 923-936,
558 doi:10.1144/0016-76492007-026.

559 Lunt, D.J., Flecker, R., Valdes, P.J., Salzmann, U., Gladstone, R. Haywood, A.M., 2008, A
560 methodology for targeting palaeo proxy data acquisition: A case study for the terrestrial
561 late Miocene. *Earth and Planetary Science Letters*, 271, 53-62.

562 Mannen, K., 2006, Total grain size distribution of a mafic subplinian tephra, TB-2, from the
563 1986 Izu-Oshima eruption, Japan: An estimation based on a theoretical model of tephra
564 dispersal. *J. Volcanol., Geotherm. Res.* 155, 1-17, doi:10-1016/j.volgeores.2006.02.004.

565 Mannen, K., Ito, T., 2007, Formation of scoria cone during explosive eruption at Izu-Oshima
566 volcano, Japan. *Geophys. Res. Lett.* 34 (L18302), doi:10.1029/2007GL030874.

567 Mastin, L.G., 2007, A user-friendly one-dimensional model for wet volcanic plumes.
568 *Geochemistry Geophysics Geosystems* 8 (3), doi:10.1029/2006GC001455.

569 Oman, L., Robock, A., Stenchikov, G.L., Thordarson, Th., Koch, D., Shindell, D.T., Gao, C.,
570 2006a, Modeling the distribution of the volcanic aerosol cloud from the 1783–1784 Laki
571 eruption. *J. Geophys. Res.* 111 (D12209), doi:10.1029/2005JD006899.

572 Oman, L., Robock, A., Stenchikov, G.L., Thordarson, Th., 2006b, High-latitude eruptions cast
573 shadow over the African monsoon and the flow of the Nile. *Geophys. Res. Lett.* 33
574 (L18711), doi:10.1029/2006GL027665.

575 Pope, V.D., Gallani, M.L., Rowntree, P.R., Stratton, R.A., 2000, The impact of new physical
576 parameterizations in the Hadley Centre Climate model: HadAM3. *Climate Dynamics*, 16,
577 123-146.

578 Pound, M.J., 2012, Middle to Late Miocene terrestrial biota and climate. PhD thesis, University
579 of Leeds.

580 Pound, M.J., Haywood, A.M., Salzmann, U., Riding, J.B., Lunt, D.J., Hunter, S.J., 2011, A
581 Tortonian (Late Miocene, 11.61-7.25 Ma) global vegetation reconstruction.
582 *Palaeogeography, Palaeoclimatology, Palaeoecology*, 300, 29-45.

583 Resnick, R., Halliday, D., 1977, *Physics I*, Third Edition. John Wiley and Sons, New York.

584 Robock, A., 2000, Volcanic eruptions and climate. *Rev. Geophys.* 38 (2), 191 - 219.

585 Schmidt, A., Carslaw, K.S., Mann, G.W., Wilson, M, Breider, T.J., Pickering, S.J., Thordarson,
586 T., 2010, The impact of the 1783-1784 AD Laki eruption on global aerosol formation
587 processes and cloud condensation nuclei. *Atmos. Chem. Phys.* 10, 6025-6041, [doi:](https://doi.org/10.5194/acp-10-6025-2010)
588 [10.5194/acp-10-6025-2010](https://doi.org/10.5194/acp-10-6025-2010).

589 Schmidt, A., Thordarson, Th., Oman, L.D., Robock, A., Self, S., 2012, Climatic impact of the
590 long-lasting 1783 Laki eruption: Inapplicability of mass-independent sulfur isotopic
591 composition measurements. *J. Geophys. Res.* 117 (D23116), doi:10.1029/2012JD018414.

592 Schmidt, A., Fristad, K., Elkins-Tanton, L., 2014, *Volcanism and Global Environmental Change*,
593 Cambridge University Press, 310 pp.

594 Self, S., Keszthelyi, L., Thordarson, Th., 1998, The importance of pahoehoe. *Ann. Rev. Earth*
595 *Plan. Sci.* 26, 81 - 110.

596 Self, S., Gertisser, R., Thordarson, Th., Rampino, M.R., Wolff, J.A., 2004, Magma volume,
597 volatile emissions, and stratospheric aerosols from the 1815 eruption of Tambora.

598 Geophys. Res. Lett. 31 (L20608), doi:10.1029/2004GL020925.

599 Self, S., Thordarson, Th., Widdowson, M., 2005, Gas fluxes from flood basalt eruptions.
600 Elements (Quebec) 1 (5), doi:10.2113/gselements.1.5.283.

601 Self, S., Widdowson, M., Thordarson, Th., Jay, A.E., 2006, Volatile fluxes during flood basalt
602 eruptions and potential effects on the global environment. Earth Plan. Sci. Letts. 248, 518
603 – 532.

604 Self, S., Schmidt, A., and Mather, T.A., 2014, Emplacement characteristics, timescales, and
605 volatile release rates of continental flood basalt eruptions on Earth, in Keller, G., and
606 Kerr, A., eds., Volcanism, Impacts, and Mass Extinctions: Causes and Effects:
607 Geological Society of America Special Paper 505, doi:10.1130/2014.2505(16).

608 Sharma, K., Blake, S., Self, S., Kreuger, A.J., 2004, SO₂ emissions from basaltic eruptions, and
609 the excess sulfur issue. Geophys. Res. Lett. 31 (L13612), doi:10.1029/2004GL019688.

610 Smithsonian Institution, 1984, Mauna Loa. Scientific Event Alert Network (SEAN) Bulletin 9
611 (3), 2-9.
612 [http://www.volcano.si.edu/volcano.cfm?vn=332020&bgvn=1&rnum=region13&snum=h](http://www.volcano.si.edu/volcano.cfm?vn=332020&bgvn=1&rnum=region13&snum=hawaii&wvol=maunaloa&tab=1#sean_0903)
613 [awaii&wvol=maunaloa&tab=1#sean_0903](http://www.volcano.si.edu/volcano.cfm?vn=332020&bgvn=1&rnum=region13&snum=hawaii&wvol=maunaloa&tab=1#sean_0903).

614 Smithsonian Institution, 1986, Izu-Oshima. Scientific Event Alert Network (SEAN) Bulletin 11
615 (11), [http://www.volcano.si.edu/world/volcano.cfm?vnum=0804-](http://www.volcano.si.edu/world/volcano.cfm?vnum=0804-01=&volpage=var#sean_1111)
616 [01=&volpage=var#sean_1111](http://www.volcano.si.edu/world/volcano.cfm?vnum=0804-01=&volpage=var#sean_1111).

617 Sparks, R.S.J., and Pinkerton, H., 1978, Effect of degassing on rheology of basaltic lava.
618 Nature, 276, 385-386.

- 619 Sparks, R.S.J., Bursik, M., Carey, S.N., Gilbert, J.S., Glaze, L.S., Sigurdsson, H., Woods, A.W.,
620 1997, *Volcanic Plumes*. John Wiley, New York.
- 621 Stothers, R.B., 1989, Turbulent atmospheric plumes above line sources with an application to
622 volcanic fissure eruptions on the terrestrial planets. *J. Atmos. Sci.* 46 (17), 2662-2670.
- 623 Stothers, R.B., Wolff, J.A., Self, S., Rampino, M.R., 1986, Basaltic fissure eruptions, plume
624 heights, and atmospheric aerosols. *Geophys. Res. Lett.* 13, 725-728.
- 625 Sumner, J.M., 1998, Formation of clastogenic lava flows during fissure eruption and scoria cone
626 collapse: The 1986 eruption of Izu-Oshima volcano, eastern Japan. *Bull. Volcanol.* 60,
627 195-212.
- 628 Swanson, D.A., Wright, T.L., Helz, R.T., 1975, Linear vent systems and estimated rates of
629 magma production and eruption for the Yakima Basalt on the Columbia Plateau. *Am. J.*
630 *Sci.* 275, 877-905.
- 631 Thordarson, Th., Self, S., 1993, The Laki (Skaftár Fires) and Grímsvötn eruptions in 1783-1785.
632 *Bull. Volcanol.* 55, 233-263.
- 633 Thordarson, Th., Self, S., 1996, Sulfur, chlorine and fluorine degassing and atmospheric loading
634 by the Roza eruption, Columbia River Basalt Group, Washington, USA. *J. Volcanol.*
635 *Geotherm. Res.* 74, 49-73.
- 636 Thordarson, Th., Self, S., 1998, The Roza Member, Columbia River Basalt Group: Gigantic
637 pahoehoe lava flow field formed by endogenous processes? *J. Geophys. Res.* 103,
638 27,411-27,445.
- 639 Thordarson, Th., Self, S., 2003, Atmospheric and environmental effects of the 1783-1784 Laki

640 eruption: A review and reassessment. *J. Geophys. Res.* 108(D1),
641 doi:10.1029/2001JD002042.

642 Thordarson, Th., Self, S., Oskarsson, N., Hulsebosch, T., 1996, Sulfur, chlorine, and fluorine
643 degassing and atmospheric loading by the 1783-1784 AD Laki (Skaftár Fires) eruption in
644 Iceland. *Bull. Volcanol.* 58, 205 - 225.

645 Thordarson Th., Self, S., Miller, D.J., Larsen, G., Vilmundardottir, E.G., 2003, Sulfur release
646 from flood lava eruptions in the Veidevotn, Grímsvötn, and Katla volcanic systems,
647 Iceland, in: Oppenheimer, C., Pyle, D.M., Barclay, J., (Eds), *Volcanic Degassing*. *Geo.*
648 *Soc., Lond., Special Publications* 213, 103-123.

649 Timmreck, C., 2012, Modeling the climatic effects of large explosive volcanic eruptions. *Wiley*
650 *Interdisciplinary Reviews: Climate Change* 3, 545-564, doi:10.1002/wcc192.

651 Van Dop, H., Van As, D., Van Herwijnen, A., Hibberd, M., Jonker, H., 2005, Length scales of
652 scalar diffusion in the convective boundary layer: Laboratory observations. *Boundary-*
653 *Layer Met.* 116, doi:10.1007/s10546-004-2165-1.

654 Vergnolle, S., Mangan, M., 2000, Hawaiian and Strombolian eruptions, in: Sigurdsson, H. (Ed.),
655 *Encyclopedia of Volcanoes*. Academic Press, San Diego, CA, 447-461.

656 Walker, G.P.L., Self, S., Wilson, L., 1984, Tarawera 1886, New Zealand – A basaltic plinian
657 fissure. *J. Volcanol. Geotherm. Res.* 21, 61-78.

658 Wignall, P.B., 2001, Large igneous provinces and mass extinctions, *Earth-Science Revs.*, 53 (1-
659 2), 1-33, doi:10.1016/S0012-8252(00)00037-4.

660 Wolfe, E.W., 1988, The Pu`u `Ō`ō eruption of Kilauea volcano, Hawaii: Episodes 1 through 20,

661 January 3, 1983, through June 8, 1984. U.S. Geol. Surv. Prof. Pap. 1463, 251 pp.

662 Wolfe, E.W., Neal, C.A., Banks, N.G., Duggan, T.J., 1988, Geologic observations and
663 chronology of eruptive events. U.S. Geol. Surv. Prof. Pap. 1463, 1-98.

664 Woods, A.W., 1988, The fluid dynamics and thermodynamics of eruption columns. Bull.
665 Volcanol. 50, 169-193.

666 Woods, A.W., 1993a, A model of the plumes above basaltic fissure eruptions. Geophys. Res.
667 Letts 20 (12), 1115 – 1118.

668 Woods, A.W., 1993b, Moist convection and the injection of volcanic ash into the atmosphere. J.
669 Geophys. Res. 98 (B10), 17627 – 17636.

670 World Meteorological Organization (WMO), 1957, Meteorology A Three-Dimensional Science:
671 Second Session of the Commission for Aerology. WMO Bulletin IV(4), WMO, Geneva,
672 134-138.

673

674 **Figure Captions**

675 Figure 1: Lava fountain from Pu`u `O`o on September 19, 1984. Fire fountain extends to
676 450 m high and sustains an ash and gas plume. Note how ash plume separates
677 from fountain before apex. See text for discussion. Photograph taken by C.
678 Heliker.

679 Figure 2: Maximum predicted plume heights as a function of fissure width using the Glaze
680 et al. (2011) model for a linear source geometry. In all cases shown, water vapor
681 is assumed to be the only volatile, and the initial velocity at the vent is 50 m/s.
682 Steam plume (long dash) is water vapor only at a temperature of 100 °C. Super-
683 heated steam (short dash) is water vapor only at near magmatic temperatures of
684 925 °C. 50% ash plume (solid line) assumes that the plume is made up of 50wt%
685 water vapor and 50wt% fragmented ash. This is relatively ash-poor compared to
686 typical bulk magmatic volatile amounts of 2 - 5wt%.

687 Figure 3: Maximum predicted plume heights as a function of effective gas content, n_f , in the
688 buoyant ash and gas plume. Horizontal dashed lines indicate the range of
689 observed buoyant ash plume heights (12 – 16 km ASL) during the explosive
690 phase of the 1986 Izu-Oshima basaltic fissure eruption. All cases assume an initial
691 temperature of 1075 °C and initial velocity of 100 m/s at the buoyant plume
692 source, 1000 m above the fissure vent (point of gas separation from the fire-
693 fountain, approximate 2/3 of the maximum fire-fountain height). Curves indicate
694 buoyant plumes from a circular source with diameter of 50 m (solid circles),
695 linear source with width of 4 m (open diamonds), and linear source with width of
696 16 m (solid line). For $n_f=6wt%$, plumes from linear sources 4 – 16 m wide rise to

697 heights of 13.1 – 17.4 km ASL. Assuming that the 14.7 Ma Roza eruption
698 sustained fire-fountains of similar height to Izu-Oshima, analogous buoyant
699 plumes would have reached the stratosphere at 45°N.

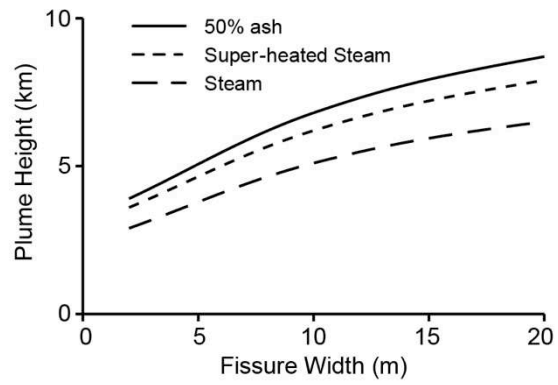
700 Figure 4: Comparison of temperature profiles used as input for the 4C plume rise model for
701 the modern atmosphere (US Standard), Miocene at 45°N (with atmospheric CO₂
702 concentrations set to 395 ppmv), and Maastrichtian at 21°S (assuming
703 atmospheric CO₂ concentrations of 1120 ppmv, which is about four times that of
704 the pre-industrial atmosphere). Arrows indicate the height of the tropopause based
705 on the World Meteorological Organization (WMO) lapse-rate criterion (WMO,
706 1957) for the Maastrichtian (20.5 km), Miocene (13 km), and US Standard (11
707 km) atmospheres.



708

709 Figure 1.

710



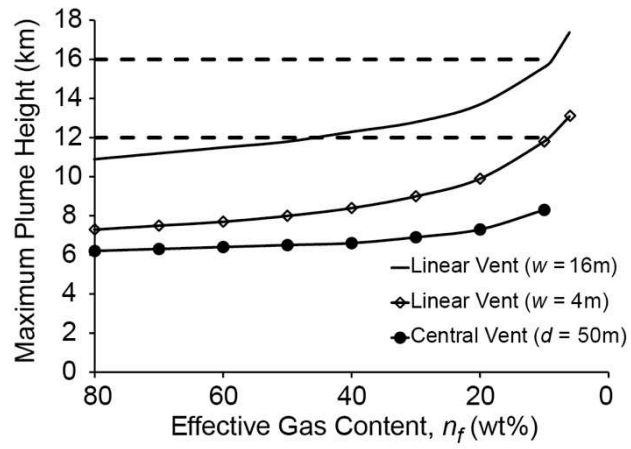
711

712

713 Figure 2.

714

715

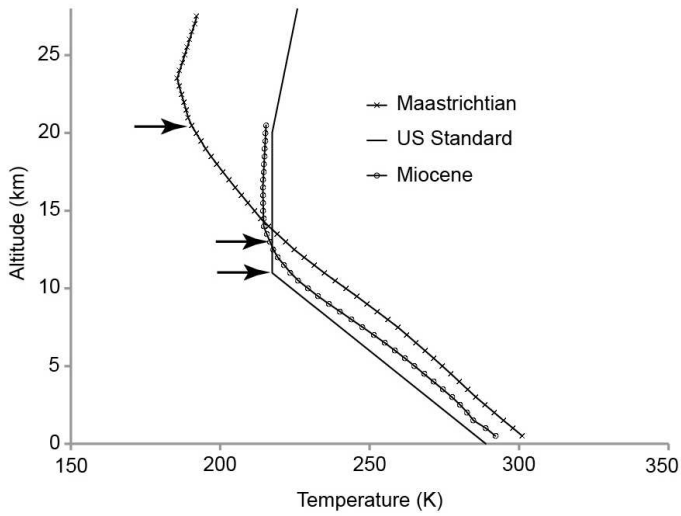


716

717

718 Figure 3.

719



720

721 Figure 4.

722

723

724

Appendix A.

Supplementary Material for: Assessing eruption column height in ancient flood basalt eruptions

<http://dx.doi.org/10.1016/j.epsl.2014.07.043>

Lori S. Glaze^a, Stephen Self^{b,c}, Anja Schmidt^d, and Stephen J. Hunter^d

^aCode 690, NASA Goddard Space Flight Center, 8800 Greenbelt Road Greenbelt, MD 20771, United States, Lori.S.Glaze@nasa.gov, ^bThe Open University, Department of Environment, Earth & Ecosystems, Walton Hall, Milton Keynes, MK7 6AA, United Kingdom, Steve.self1815@gmail.com, ^cUniversity of California, Berkeley, Earth and Planetary Science, 307 McCone Hall, Berkeley, CA 94720-9980, United States, ^dUniversity of Leeds, School of Earth and Environment, Leeds, LS2 9JT, United Kingdom, A.Schmidt@leeds.ac.uk, S.Hunter@leeds.ac.uk

Appendix A

Here we provide direct comparisons of the *4C* and *Plumeria* buoyant plume rise models. *4C* is based on the approach contained in the series of Glaze et al. papers (Glaze and Baloga, 1996; Glaze et al., 1997; Glaze, 1999; Glaze and Baloga, 2002; Glaze et al., 2011). A complete definition of *4C* for circular vents is given in Glaze et al. (1997). *Plumeria* (Mastin, 2007) is a user-friendly program that is freely available through the USGS Cascade Volcano Observatory (<http://vulcan.wr.usgs.gov/Projects/Mastin/Publications/G3Plumeria/framework.html>, last accessed 15 July 2013). The plume rise physics contained in *Plumeria* are based on Woods (1988; 1993).

Both *Plumeria* and *4C* begin with mass, momentum, and thermal energy conservation and both approaches model the buoyant rise of solid ash, water vapor (magmatic and entrained), ambient air, and liquid water. Both models also include the release of latent heat during water vapor condensation. The fundamental assumption of both models is that the effects of convection and turbulence on mass conservation can be estimated through an entrainment parameter (Morton et al., 1956). Although recent work by Carazzo et al. (2008) have indicated that the entrainment parameter may be variable, a constant value has been shown by numerous studies to be adequate to first order and is assumed here. Because both modeling approaches are based on Morton et al. (1956), the basic physics are similar, and maximum plume heights predicted by both approaches are also similar.

Table A1 details predicted plume heights from *Plumeria* and *4C*. The criterion used by *Plumeria* to stop plume rise is the point at which the upward velocity drops below 1 m/s. Because *4C* typically uses a value of 10 m/s to estimate the maximum plume height, the height

Table A1. Predicted maximum plume heights from *Plumeria* and *4C*; radius=vent radius, u =bulk plume velocity, H =maximum plume height (see text for details).

radius (diameter) (m)	<i>Plumeria</i> H (km) ($u < 1$ m/s)	<i>Plumeria</i> H (km) ($u < 10$ m/s)	<i>4C</i> H (km) ($u < 10$ m/s)	Delta (km)	% diff
20 (40)	11.4	11.3	10.5	0.8	7.6%
50 (100)	15.4	15.3	14.6	0.7	4.8%
100 (200)	19.6	19.6	18.7	0.9	4.8%
150 (300)	23.1	23	22	1	4.5%
200 (400)	26	26	24.9	1.1	4.4%
250 (500)	28.6	28.5	27.5	1	3.6%

predicted by *Plumeria* when velocity drops below 10 m/s is given in column three. The fourth column shows the predicted plume heights with a cutoff value of 10 m/s using *4C*.

In all cases, the following input parameters are assumed: Ambient air temperature at the vent =15.86 C, Tropospheric lapse rate =-6.5 K/km, vent elevation=0 km, relative humidity =0%, tropopause elevation =11 km, eruption velocity=300 m/s, eruption temperature =1000 K, magmatic volatile content (assumed to be water) =3wt%. For consistency with values stated in Mastin (2007), a specific heat for the solid particles of 1100 J/K/kg (Sparks, 1986) is used in *4C*. *4C* uses the US Standard Atmosphere to define ambient temperature and pressure profiles, which has a stratospheric lapse rate of 1.053 K/km between 11–20 km, and a lapse rate of 2.5 between 20-32 km. The standard *Plumeria* input only allows use of a single lapse rate in the stratosphere. As a result, plumes that rise higher than 20 km may have additional discrepancies introduced by atmospheric temperature.

Maximum plume heights predicted by *Plumeria* and *4C* differ by only a few percent (Table A1, column 6), with that difference decreasing as the plume size increases. There are two significant ways in which the models differ. First, as discussed in Glaze and Baloga (1996), the thermal energy conservation of Woods (1988) is inconsistent with the rest of the system of conservation equations. Glaze et al. (1997) define the basic thermal energy, without latent heat, as

$$\frac{d}{dz}(\rho_B u r^2 C_B \theta) = 2\alpha \rho_a u r C_a \theta_a - \rho_a u r^2 g$$

where z is the vertical variable, ρ_a and ρ_B are bulk densities of the atmosphere and plume, u is upward plume velocity, r is plume radius, C_a and C_B are specific heats of the bulk atmosphere and the plume, θ and θ_a are plume and atmosphere temperatures, and g is gravitational acceleration. For comparison, Woods (1988) defines this same thermal energy balance as

$$\frac{d}{dz}(\rho_B u r^2 C_B \theta) = 2\alpha \rho_a u r C_a \theta_a + \frac{u^2}{2} g (\rho_a - \rho_B) r^2 - \rho_a u r^2 g$$

The additional term on the right hand side of the Woods (1988) expression is not consistent with the momentum conservation equation (Glaze and Baloga, 1996). Figure A1 illustrates the impact of this difference on the bulk plume temperature as a function of height. Although, the temperature differences are small, correcting this inconsistency in *4C* results in maximum plume heights 4-7% lower than predicted by the Woods (1988) model (Glaze, 1999). Note that this one discrepancy describes all of the observed maximum plume height differences in Table A1.

Another difference between *Plumeria* and *4C* is that Woods (1988) defines the transition between the jet and buoyancy regions as the point where bulk plume density drops below ambient density. However, as noted by Glaze (1999), this transition definition results in discontinuous solutions for all variables.

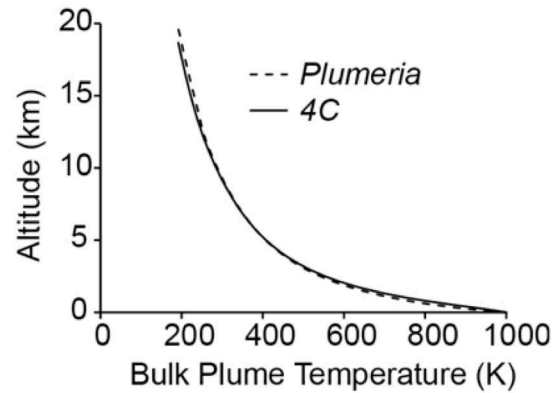


Figure A1: Comparison of bulk plume temperature as a function of altitude as estimated by the *Plumeria* and *4C* models. Both models assume a circular vent of radius 100 m, initial velocity of 300 m/s, initial temperature of 1000 K, and bulk volatile content of 3wt%. Inconsistency in the Woods (1988) thermal energy conservation equation results in small differences in the bulk plume temperature.

Alternatively, continuous solutions across the jet-buoyancy boundary (that converge at the same height above the vent) can easily be found for all variables. Figure A2 shows the transition height above the vent as a function of vent radius for both the continuous and discontinuous solutions. Requiring continuous solutions for all variables across this boundary (as dictated by physical systems) results in transition heights substantially lower than those determined using the discontinuous solution. Further, continuous solution transition heights do not vary much as a function of mass flux at the vent.

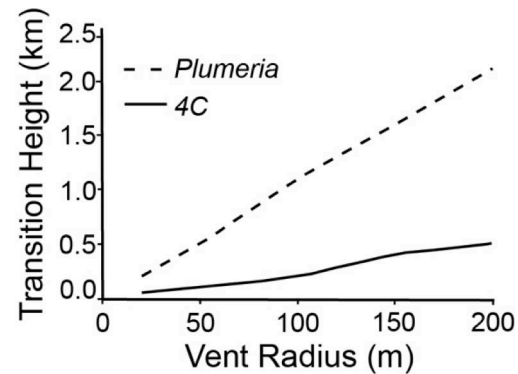


Figure A2: Figure after Glaze (1999). Comparison of heights where transition occurs between the jet- and buoyancy-driven regions for both the *Plumeria* and *4C* models. Both cases assume initial velocity of 300 m/s, initial bulk temperature of 1000 K, initial bulk volatile content of 3wt%, vent altitude of 0 km, and initial circular vent radius as shown on the x axis. The discontinuous transition employed by *Plumeria* results in an overestimate of the maximum plume height (Table A1).

References

- Carazzo, G., Kaminski, E., Tait, S., 2008, On the rise of turbulent plumes: Quantitative effects of variable entrainment for submarine hydrothermal vents, terrestrial and extra terrestrial explosive volcanism. *J. Geophys. Res.* 113, doi:10.1029/2007JB005458.
- Glaze, L.S., 1999, Transport of SO₂ by explosive volcanism on Venus. *J. Geophys. Res.* 104 (E8), 18,899 - 18,906.
- Glaze, L.S., Baloga, S.M., 1996, Sensitivity of buoyant plume heights to ambient atmospheric conditions: Implications for volcanic eruption columns. *J. Geophys. Res.* 101 (D1) 1529-1540.
- Glaze, L.S., Baloga, S.M., 2002, Volcanic plume heights on Mars: Limits of validity for convective models. *J. Geophys. Res.* 107 (E10), doi:10.1029/2001JE001830.
- Glaze, L.S., Baloga, S.M., Wilson, L., 1997, Transport of atmospheric water vapor by volcanic eruption columns. *J. Geophys. Res.* 102 (D5), 6099 – 6108.
- Glaze, L.S., Baloga, S.M., Wimert, J., 2011, Explosive volcanic eruptions from linear vents on Earth, Venus and Mars: Comparisons with circular vent eruptions. *J. Geophys. Res.* 116 (E01011), doi:10.1029/2010JE003577.
- Mastin, L.G., 2007, A user-friendly one-dimensional model for wet volcanic plumes. *Geochemistry Geophysics Geosystems* 8 (3), doi:10.1029/2006GC001455.
- Morton, B.R., Taylor, S.G., Turner, J.S., 1956, Turbulent gravitational convection from maintained and instantaneous sources. *Proc. Roy. Soc. Lond. Series A-Mathematical and Physical Sciences* 234, 1-23.
- Sparks, R.S.J., 1986, The dimensions and dynamics of volcanic eruption columns. *Bull. Volcanol.* 48, 3-15.
- Woods, A.W., 1988, The fluid dynamics and thermodynamics of eruption columns. *Bull. Volcanol.* 50, 169-193.
- Woods, A.W., 1993, Moist convection and the injection of volcanic ash into the atmosphere. *J. Geophys. Res.* 98 (B10), 17627 – 17636.